

Fig. 2 Western blot analysis of lysates extracted from E. colicells harboring the pMEx8 vector (lane 2), pME4D (lane 3), or the mutant plasmids-K123A, Y125A, N128A, S130A, Q135A, R136A, R136K, R136Q, R136D, Q139A, and E141A (lanes 4-14, respectively)-showing the 65-kDa Cryl1 toxin and small molecular fragments that cross-reacted with the Cryl1A antibodies. Lane 1 represents the molecular mass standards.

charged and five polar amino acids in helix 4 (Fig. 1B) were substituted with alanine. Most of the targeted residues, Tyr-125, Asn-128, Gln-135, Arg-136 and Gln-139, but not Lys-123, Ser-130 and Glu-141, are located at the hydrophilic surface (see Fig. 1C).

Expression of the mutant toxins in E. coli was controlled by the tac promoter. Upon addition of IPTG to mid-exponential phase cultures, all mutant toxins were predominantly produced as sedimentable inclusion bodies. Lysates were analyzed by SDS-PAGE and immunoblotting, and the protein expression level of all mutant derivatives was found to be comparable to the wild type. The 65-kDa expressed mutant proteins specifically cross-reacted with antibodies raised against the CryllA toxin (see Fig. 2). However, two relatively intense immuno-reactive bands of ca. 50 kDa and ca. 35 kDa were detected in all mutant lysates. This indicates that the expressed mutant proteins are rather sensitive to proteolytic degradation.

The solubility of mutant protein inclusions in comparison to the wild-type inclusion was assessed using a carbonate buffer, pH 9.0. The amount of 65-kDa soluble proteins in the supernatant was compared with those of the proteins initially used, in order to determine the percentage of protein solubilisation. All of the mutant inclusions were found to be soluble to some extent in this buffer, giving less than 20% solubility, which resembles closely the wild-type inclusions under similar conditions.

To determine the effect of mutations on toxicity, E. colicells that expressed each type of the mutant toxin were tested for their relative biological activity towards Aedes aegypti larvae. All of the assays were carried out in ten replicas for each sample and repeated three times; the mortality data recorded after a 24-hour incubation are shown in Fig. 3. Interestingly, only the R136A mutation resulted in a total loss of larvicidal activity, while alanine substitutions at seven other positions (K123A, Y125A, N128A, S130A, Q135A, Q139A)

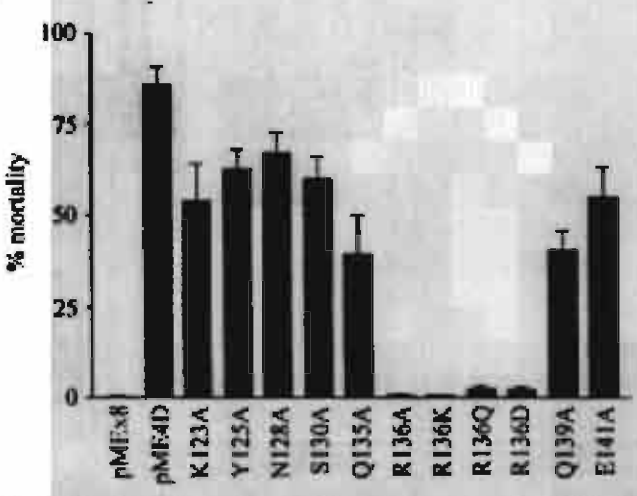


Fig. 3. Mosquito-larvicidal activities of *E. coli* cells expressing the Cryl1A wild-type textin (pME4D), or its mutants-K123A, Y125A, N128A, S130A, Q135A, R136A, R136K, R136Q, R136D, Q139A and E141A)-against *Aedes aegypti* larvae. Error bars indicate standard error of the mean from the three independent experiments.

and E141A) still retained over 50% of the wild-type activity. When this critical arginine residue at position 136 was converted to aspartate, glutamine or even to the most conserved residue for positively charged side chain, i.e. lysine, all R136 mutants (R136D, R136Q and R136K) were shown to be nontoxic to mosquito larvae (see Fig. 3). These results could imply the requirement for a specific structure of the positive side chain at this position. Perhaps Arg-136, which is likely to face the pore lumen, could interact with an aqueous environment, and somehow stabilize the functional pore. However, the precise function of this residue remains to be elucidated.

Protein expression levels and solubility of the inclusions suggested that the complete loss of toxicity observed for the R136A mutant is least likely to be caused by misfolding of the protein. Taken together, our results indicate that Arg-136 is a critical residue involved in CryllA toxin activity. The data further support our previous findings that Arg-158 in 04 played a crucial role in toxicity of the 130-kDa Cry4B toxin. since the single alanine substitution at this residue almost completely abolished its activity towards mosquito larvae (Sramala et al., 2001). In addition, results reported by other workers revealed that an arginine residue at position 131 in 04 is important for toxicity of both the lepidopteran-specific Cryl Aa and Cryl Ac toxins (Kurner and Aronson, 1999; Masson et al., 1999). Two other negatively charged residues (Glu-129 and Asp-136) of Cry1Aa were also shown to be critical in the passage of ions through the pore (Masson et al., 1999).

Companisons of structural models among Cry11A, Cry4B, and Cry1An suggest that, although Arg-136 of Cry11A is located on the opposite side of helix 4 relative to Arg-158 of Cry4B or Arg-131 of Cry1Aa, all of these three critical

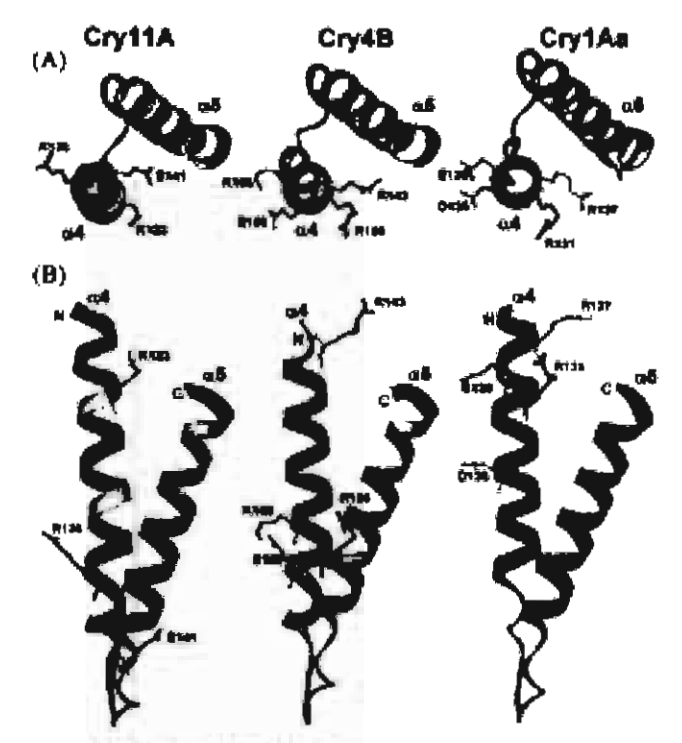


Fig. 4. (A) Top and (B) side views of amino acid arrangement in helix 4 together with the relative position of helix 5 in 3D models of Cry11A and Cry4B built by homology modeling and the Cry1Aa crystal structure. The labeled residues, shown in red and yellow, indicate the critical arginine residues and other charged positions, respectively. The structures were prepared using Weblab viewer (Molecular Simulations Inc.).

residues are oriented on the side of belix 4, which is furthest away from helix 5 (see Fig. 4A). It should be noted that Arg-136 and Arg-158, in both of the dipteran-specific toxins, are situated near the C-terminal end of helix 4, while Arg-131 of the lepidopteran-specific Cry IAa toxin is located furthest from the C-terminus of this helix (Fig. 4B). Differences in the location of these critical residues may conceivably reflect the diversity in the channel architecture for each group of insect-specific Cry toxins. Further studies are required to elucidate the role of these positively charged residues in helix 4, to discover whether they are involved in the passage of ions through the pore.

Acknowledgments We are grateful to Prof. Prapon Wilairat for the helpful comments. We thank U. Chamama for the excellent technical support with DNA sequencing, as well as A. Nirachanon and S. Shimwai for technical assistance. This work was supported in part by the National Science and Technology Development Agency of Thailand and the Thailand Research Fund.

References

Angsuthanasombat, C., Crickmore, N. and Ellar, D. J. (1993)
Effects on toxicity of eliminating a cleavage site in a predicted

interhelical loop in Bacillus thuringiensis CryIVB deltaendotoxin. FEMS Microbiol. Lea. 111, 255-261.

Buttcher, V., Ruhlmunn, A. and Cramer, F. (1990) Improved single-stranded DNA producing expression vectors for protein munipulation in Escherichia coli, Nucleic Acids Res, 18, 1075.

Crickmore, N., Zeigler, D. R., Feitelson, J., Schnepf, E., Van Rie, J., Lereclus, D., Baum, J. and Dean, D. H. (1998) Revision of the nomenclature for the *Bacillus thuringleusis* pesticidal crystal proteins. *Microbiol. Mol. Biol. Rev.* 62, 807-813.

de Maagd, R. A., Bravo, A. and Crickmore, N. (2001) How Bacillus thuringiousis has evolved specific toxins to colonize the insect world. Trends Gener. 4, 193-199.

Gazit, E., La Rocca, P., Sansom, M. S. and Shai, Y. (1998) The structure and organization within the membrane of the helices composing the pore-forming domain of *Bacillus thuringiensis* delta-endotoxin are consistent with an "umbrella-like" structure of the pore. *Proc. Natl. Acad. Sci. USA* 95, 12289-12294.

Gerber, D. and Shai, Y. (2000) Insertion and organization within membranes of the delta-endotoxin pore-forming domain, helix 4-loop-helix 5, and inhibition of its activity by a mutant helix 4 pepcide. J. Biol. Chem. 275, 23602-23607.

Grochulski, P., Masson, L., Borisova, S., Pusztai-Carey, M., Schwartz, J. L., Brousseau, R. and Cygiez, M. (1995) Bacillus thuringiensis CrylA(a) insecticidal toxin: crystal structure and channel formation. J. Mol. Biol. 254, 447-464.

Guerrea, L. and Bravo, A. (1999) The oligomeric state of Bacillus thuringiensis Cry toxins in solution. Biochem. Biophys. Acta 1429, 342-350.

Hofte, H. and Whiteley, H. R. (1989) Insecticidal crystal proteins of Bacillus thuringiensis. Microbiol. Rev. 53, 242-255.

Knowles, B. H. and Ellar, D. J. (1987) Colloid-esmotic lysis is a general feature the mechanism of action of Bacillus thuringiensis δ-endotoxins with different insect specificity. Biochem. Biophys. Acta 924, 509-518.

Knowles, B. H. (1994) Mechanism of action of Bacillus thuringiensis insecticidal 8-endotoxins. Adv. Insect. Physiol. 24, 275-308.

Kumar, A. S. and Aroason, A. L (1999) Analysis of mutations in the pore-forming region essential for insecticidal activity of a Bacillus thurlugiensis delta-endotoxin. J. Bacteriol. 181, 6103-6107.

Li, J. D., Carroll, J. and Ellar, D. J. (1991) Crystal structure of insecticidal delta-endotoxin from *Bacillus shuringiensis* at 2.5 Å resolution. *Nature* 353, 815-821.

Masson, L., Tubashnik, B. E., Liu, Y. B., Brousseau, R. and Schwartz, J. L. (1999) Helix 4 of the Bacillus thur inginesis: Cryl Aa toxin lines the lumen of the ion channel. J. Biol. Chem. 274, 31996-32000.

Nunez-Valdez, M.-E., Sanchez, J., Lina, L., Guerreza, L. and Bravo, A. (2001) Structural and functional studies of or-helix 5 region from *Bacillus thuringiensis* CrylAb 8-endotoxins. *Biochimi. Biaphys. Acta* 1546, 122-133.

Puntheeranurak, T., Lectacheewa, S., Katzenmeier, G., Krittanai, C., Panyim, S. and Angauthanascrobat, C. (2001) Expression and biochemical characterization of the Bacillus thuringiensis Cty4B 0.1-0.5 pone-forming fragment. J. Biochem. Mol. Biol. (in press).

Schnepf, E., Crickmore, N., Van Rie, J., Lerectus, D., Baum, J., Feitelson, J., Zeigler, D. R. and Dean, D. H. (1998) Bacillus thuringiensis and its pesticidal crystal proteins. Microbiol. Mal. Biol. Rev. 62, 775-806.

Schwartz, J. L., Juteau, M., Grochulski, P., Cygler, M., Prefontaine, G., Brousseau, R. and Masson, L. (1997) Restriction of intramolecular movements within the Cry1Aa toxin molecule of Bacillus thuringiensis through disulfide bond engineering, FEBS Lett. 410, 397-402.

Sramala, I., Uswithya, P., Chanama, U., Leetachewa, S., Kristanai, C., Katzenmeier, G., Panyim, S. and Angsuthanasombat, C. (2000) Single proline substitutions of selected helices of the Bacillus thuringiensis Cry4B toxin affect inclusion solubility and larvicidal Activity. J. Biochem. Mol. Biol. Biophys. 4, 187-193.

Srumala, I., Lectachewa, S., Krittanai, C., Katzenmeier, G., Panyim, S. and Angsuthanasombat, C. (2001) Screening charged residues in helix 4 of the Bacillus thuringiensis Cry4B 10xin reveals one critical residue for larvicidal activity. J. Biochem. Mol. Biol. Biophys. (in press).

Ulawithya, P., Krittanai, C., Katzenmeier, G., Lectachewa, S.,

Panyim, S. and Angsuthanasombat, C. (1999) 3D models for Bacillus thuringiensis Cry4A and Cry4B insecticidal proteins based on homology modeling. Abstract 32rd Meeting. Society for Invertebrate Pathology, Irvine, USA, p. 75.

Uswithya, P., Tuntitippawan, T., Katzesineier, G., Panyim, S. and Angsuthanasombut, C. (1998) Effects on larvicidal activity of single proline substitutions in O3 or O4 of the Bacillus thuringiensis Cry4B toxin. Blochem. Mol. Biol. Int. 44, 825-832.

Von Tersch, M. A., Slatin, S. L., Kulesza, C. A. and English, L. H. (1994) Membrane-permeabilizing activities of Bacillus thurungiensis coleopteran-active toxin CryllIB2 and CryllIB2 domain I peptide. Appl. Emviron. Microbiol. 60, 3711-3717.

Walters, F. S., Slatin, S. L., Kulesza, C. A. and English, L. H. (1993) Ion channel activity of N-terminal fragments from CrylA(c) delta-endotoxin. *Biochem. Biophys. Res. Commun.* 196, 921-926.

RESEARCH

Specific Mutations Within the α4–α5 Loop of the *Bacillus thuringiensis* Cry4B Toxin Reveal A Crucial Role for Asn-166 and Tyr-170

Yodsoi Kanintronkul, Issara Sramala, Gerd Katzenmeier, Sakol Panyim, and Chanan Angsuthanasombat*

Abstract

The widely accepted model for toxicity mechanisms of the Bacillus thuringiensis Cry δ-endotoxins suggests that belices α4 and α5 form a helix-loop-helix hairpin structure to initiate membrane insertion and pore formation. In this report, alanine substitutions of two polar amino acids (Asn-166 and Tyr-170) and one charged residue (Glu-171) within the α4-α5 loop of the 130-kDa Cry4B mosquito-larvicidal protein were initially made via polymerase chain reaction-based directed mutagenesis. As with the wild-type toxin, all of the mutant proteins were highly expressed in Escherichia coli as inclusion bodies upon isopropyl-β-p-thiogalactopyranoside induction. When E. coli cells expressing each mutant toxin were assayed against Aedes aegypti mosquito larvae, the activity was almost completely abolished for N166A and Y170A mutations, whereas E171A showed only a small reduction in toxicity. Further analysis of these two critical residues by induction of specific mutations revealed that polarity at position 166 and highly conserved aromaticity at position 170 within the α4-α5 loop play a crucial role in the larvicidal activity of the Cry4B toxin.

Index Entries: Aromaticity; Bacillus thuringiensis; δ-endotoxins, mutagenesis; larvicidal activity; polarity.

1. Introduction

During sporulation, the gram-positive bacterium Bacillus thuringiensis (Bt) produces intracellular crystalline inclusions consisting of one or more insecticidal proteins known as δ -endotoxins (1). These cytoplasmic inclusions, which are released together with the bacterial spore upon completion of sporulation, are specifically toxic to several orders of insect larvae including Lepidoptera (butterflies and moths), Coleoptera (beetles), Diptera (mosquitoes and flies), and Hymenoptera (wasps and bees) (1-3). The Bt δ -endotoxins can be classified into the two families of Cry (crystal) and Cyt (cytolytic) toxins, in accordance with the recently revised nomenclature based on their amino-acid sequence identity (4). For instance,

one of the four major insecticidal proteins produced by Bt subsp. israelensis has been classified as Cry4B, and is highly active against mosquito larvae of the genera Aedes and Anopheles (1,4).

The Bi δ-endotoxins are present in the native crystalline inclusions as insoluble inactive protoxins. Upon ingestion by susceptible larvae, the protoxin inclusions are solubilized in the larval midgut and activated by midgut proteases. It is believed that the activated toxins first bind to a specific receptor located on apical membranes of midgut epithelial cells of the target insect larvae. Subsequently, the toxins insert into the membrane in an irreversible binding step, and disrupt the permeability of the midgut cell membranes, resulting in a net influx of ions and water that

*Author to whom all correspondence and reprint requests should be addressed: Laboratory of Molecular Biophysics, institute of Molecular Biology and Genetics, Mahidol University, Salaya Campus, Nakompathom 73170, Thailand. E-mailisten@mahidoLac.th

Molecular Biolechnology (17003 Humana Press Inc. All rights of any nature whatseever reserved, 1073-6085/2003/24-1/11-19/520:00

leads to osmotic cell lysis (5). However, the exact nature of this toxicity process at the molecular level, especially in the step of membrane insertion and lytic pore-formation, is still not clearly understood. Knowledge of the pore-forming structure within the lipid membranes could therefore advance understanding of the precise mode of action of these toxins, and would facilitate the design of more potent toxins.

To date, tertiary structures of four different Cry toxins, Cry I Aa (6), Cry 2 Aa (7), Cry 3 Aa (8), and Cry3Bb (9), have been determined by X-ray crystallography. Despite the differences in their insect specificity and the comparatively low amino-acid sequence identity between these proteins, the structures of all four of them display a high degree of overall similarity. A homology-based 3D model of the 65-kDa activated Cry4B toxin suggests that this mosquitocidal protein would fold into a structure similar to known crystal structures with a three-domain organization (10). The N-terminal domain I is composed of seven a helices in which the relatively hydrophobic helix as is encircled by six other amphipathic helices (6-9). That this domain is clearly equipped for membrane insertion and pore formation has been supported by various studies demonstrating that the isolated helical fragment of different Cry toxins is responsible for pore/ ion-channel-forming activity (11-13).

A molecular mechanism of membrane insertion and pore formation of the Cry \delta-endotoxins has been proposed in an "umbrella model" (14). In this model, the 04 and 0.5 helices form a helical hairpin to initiate membrane penetration upon specific receptor binding in which a structural rearrangement of the toxin occurs. After insertion of this hairpin, the other helices spread over the membrane surface in a step that is followed by oligomerization of the toxin in the membranes. Currently, this proposed model is supported by a number of experiments demonstrating the functional role of 0.4 and a5 in the loxicity of different Cry toxins. Evidence suggests than 0.4 is oriented to face the pore lumen and is involved in channel function, whereas \$\alpha\$5 appears to be in contact with the lipid membranes and plays a role in toxin oligomerization (15-17). In addition, membrane permeation studies found that the $\alpha4$ -loop- $\alpha5$ hairpin was extremely active as compared with the isolated helices or their mixtures, indicating that the loop is needed for efficient insertion into the lipid membranes (18).

Previously, we have made proline substitutions in five helices (i.e., $\alpha 3$, $\alpha 4$, $\alpha 5$, $\alpha 6$, and $\alpha 7$) of the 130-kDa Cry4B toxin, and found that helices \alpha4 and 0.5 are important determinants of larvicidal activity (19,20) and likely to be involved in membrane pore formation. Further investigation by charged-to-alanine scanning mutagenesis in helix 4 revealed that the specific structure for the positively charged side chain of Arg-158 is critically involved in the toxic activity of Cry4B (21). As an extension of the previous studies together with the proposed umbrella model, we hypothesized that when the loop connecting a4 and a5 initially inserts into the membrane, polar or charged residues in this loop may interact with ions and water molecules. These residues could play a critical role in the toxicity of Cry4B. To test this hypothesis, we created a number of Cry4B mutants in which Asn-166, Tyr-170, or Glu-171 in the α4-α5 loop was altered. The results revealed that polarity of Asn-166 and aromaticity of Tyr-170 residues are essential for larvicidal activity of the Cry4B toxin.

2. Materials and Methods

2.1. Plasmids and Site-Directed Mutagenesis

The recombinant pMU388 plasmid encoding the 130-kDa Cry4B toxin, which has been cloned from Br subsp. israelensis into pUC12 vector (22), was used as a template for site-directed mutagenesis. In order to substitute Asn-166, Tyr-170, and Glu-171 with alanine and other amino acids, 13 pairs of complementary mutagenic oligonucleotide primers (Table 1) were designed and purchased from Genset Inc. (Singapore). All mutant plasmids were generated by polymerase chain reaction (PCR) using high-fidelity Pfu DNA polymerase according to the procedure of the Quick-Change™ Mutagenesis Kit (Stratagene). Each mutant plasmid was then confirmed in the mutated region by DNA sequencing, using an ABI prism 377 automated sequencer (PerkinElmer).

Table 1
Complementary Primers for Substituting a Code Residue with Different Amino Acids

Primer	Sequence	Restriction site
10	A	
N166A-f:	5'-CGAGAGACTGCAGTTTATTTTAGCGCATTAGTAGGT-3'	Psri
N166A-r:	5'-ACCTACTAATGCGCTAAAATAAACTGCAGTCTCTCG-3'	- 4
	C	
A166C-1:	5'-GACTGCAGTTTATTT <u>CAGCTG</u> TTTAGTAGGTTATG-3'	PvaH
A166C-r:	5'-CATAACCTACTAAA <u>CAGCTG</u> AAATAAACTGCAGTC-3'	
ALLEGE E	D	
N166D-f:	5'-CGAGAGA <u>CAGCTG</u> TTTATTTTAGCGATTTAGTAGG-3'	Hwr 4
N166D-r:	5'-CCTACTAAATCGCTAAAATAAA <u>CAGCTG</u> GTCTCTCG-3'	
NII COO	Q Q	
N166Q-f:	5'-CGAGAGACCGCAGTATACTTTAGCCAATTAGTAGG-3'	Accl
N166Q-r:	5'-CCTACTAA'TTGGCTAAAGTATACTGCGGTCTCTCG-3'	
ALLESTO E	R CARACTER CONTRACTOR OF THE C	*** *
N166R-f:	5'-GAGACCGCAGTTTATTTT <u>TCTAGA</u> TTAGTAGGTTATG-3'	Xbal
N166R-r:	5'-CATAACCTACTAA <u>TCTAGA</u> AAAATAAACTGCGGTCTC-3'	
MICETE		D \$17
N1661-f:	5'-GTTTATTTTAGCATCCTGGTAGGTTATG-3'	BsiNI
N166I-r:	5'-CATAACCTA <u>CCAGGA</u> TGCTAAAATAAAC-3'	
3/170 A 6	A 5'-GACCGCAGTATACTTTAGCAACTTAGTAGGTGCTGAATTATTG-3'	A self
Y170A-f: Y170A-r:	5'-CAATAATTCAGCACCTACTAAGTTGCTAAAGTATACTGCGGTC-3'	
1 (7025-1:	3-CANIANTICAGCACCTACTAAGTTGCTAAAGTATACTGCGGTC-3	
V130D 6	D 5'-GCAGTTTATTTTAGCAAC <u>CTG</u> GTAGGT <u>G</u> ATGAATTATTG-3'	BstNI
Y170D-f: Y170D-r:	5'-CAATAATTCATCACCTACCAGGTTGCTAAAATAAACTGC-3'	DMINI
11700-1	3-CANTANTICATEACCTACCTACCAGOTTOCTAAAATAAACTOC-3	
V1200 f	R	Ned
Y 170R-f: Y 170R-r:	5'-GCAGTTTATTTTAGCAACTTAGTAGG <u>TCGCGA</u> ATTATTG-3' 5'-CAATAAT <u>TCGCGA</u> CCTACTAAGTTGCTAAAATAAACTGC-3'	TANAKI
TIVOR-E	3-CANTANTICGCGACTACTAGTTGCTAAAATAAACTGC-3	
Y170L-f:	5' GCAACTTAGTAGG <u>TCTAGA</u> ATTATTGTTATTACC-3'	Xbal
Y170L-r:	5'-GGTAATAACAATAAT <u>TCTAGA</u> CCTACTAAGTTGC-3'	
	F	***
Y170F-f:	5' GCAACTTAGTAG <u>GATTC</u> GAAT[ATTGTTATTACC-3'	Hinfl
Y170F-r:	5'-GGTAATAACAATAATTC <u>GAATC</u> CTACTAAGTTGC-3'	
	W	
Y170W-f.	S'-GCAGTTTATTT <u>TTCGAA</u> CTTAGTAGGTTGGGAATTATTG-3'	B st 31
Y170W-r:	5'-CAATAATTCCCAACCTACTAAG <u>TTCGAA</u> AAATAAACTGC-3'	
uniti -		
E171A-f:	5'-TATTTTAGCAACCTGGTAGGTTATGCATTATTGTTA-3'	B.stNI
E171A-r:	S'-TAACAATAATGCATAACCTACCAGGTTGCTAAAATA-3'	

[&]quot;Mutated nucleotide residues are shown as holdiage. Mutated amino acids are shown on top of each pair of primers, introduced restriction-cazyme recognition sites are underlined.

2.2. Toxin Expression, Solubilization and Proteolytic Activation

The wild-type and $\alpha 4$ - $\alpha 5$ loop Cry4B mutant toxins were expressed in E. coli strain JM109 under control of the LacZ promoter. Cells were grown in a Luria Broth medium containing 100 μg/mL ampicillin until the OD₆₀₀ of the culture reached 0.3-0.5. After the addition of isopropylβ-D-thiogalactopyranoside (IPTG) to a final concentration of 0.1 mM, incubation was continued for another 4 h. Protein expression was analyzed by sodium dodecyl sulfate- (13% w/v) polyacrylamide gel electrophoresis (SDS-PAGE). E. coli cells expressing each mutant Cry4B toxin as cytoplasmic inclusion bodies were harvested by centrifugation, resuspended in distilled water, and disrupted in a French Pressure Cell at 10,000 psi. The crude lysates were centrifuged at 5,000g for 20 min and the pellets obtained were washed 3 times in distilled water by sonication. Protein concentrations were determined by using a protein microassay (Bio-Rad), with bovine serum albumin fraction V (Sigma) as a standard. Protoxin inclusions were solubilized in 50 mM Na₂CO₃, pH 9.0 and incubated at 37°C for 1 h as previously described (19). After centrifugation for 10 min, the supernatants were analyzed via SDS-PAGE in comparison with the inclusion suspension. To test the stability of the mutant toxins, the solubilized mutant and wild-type toxins were incubated with tolyisulfonyl phenylalanyl chloromethyl ketone (TPCK)-treated trypsin at a ratio of 1:20, (w/w) enzyme:toxin in 50 mM Na2CO3, pH 9.0, for 16 h.

2.3. Larvicidal Activity Assays

Bioassays were performed as previously described (20), using 2-d old Aedes aegypti mosquito larvae reared from eggs that were supplied by the mosquito-rearing facility of the Institute of Molecular Biology and Genetics, Mahidol University, Nakornpathom, Thailand. About 500 larvae were reared in a container (22 × 30 × 10 cm) with approx 3 L of distilled water supplemented with a small amount of rat diet pellets. Both the rearing of larvae and the bioassays were done at room temperature (25°C). The assays were done in 1 mL of E. coli suspension (10° cells suspended in

distilled water) in a 48-well microtiter plate (11.3-mm well diameter; Costar), with 10 larvae per well and a total of 100 larvae for *E. coli* expressing each type of the Cry4B toxin. *E. coli* cells containing the pMEx8 vector were used as a negative control. Mortality was recorded after a 24-h incubation period.

3. Results and Discussion

It has recently been shown that the loop connecting the 0.4 and 0.5 helices of Cry I Ac is needed for efficient insertion of the α4-α5 helical hairpin into lipid membranes (18). As predicted from the homology-based 3D model of Cry4B, the α4-α5 loop comprises eight amino acids, of which one is charged (i.e., Glu-171) and two of which are polar (i.e., Asn-166 and Tyr-170) (10). Although Asn-166 is not conserved, both Tyr-170 and Glu-171 are structurally conserved among the known Cry toxins (see Fig. 1A,B) with the result that these loop residues could play a crucial role in Cry4B toxicity. In this study, we therefore initially generated three Cry4B loop mutants in which Asn-166, Tyr-170, and Glu-171 were substituted with alanine via PCR-based directed mutagenesis. When each mutant toxin was expressed in E. coli upon IPTG induction, all were predominantly produced as sedimentable inclusion bodies, and the protein expression level was comparable to that of the wild-type Cry4B toxin. In addition, all of the purified mutant inclusions were found to be soluble in carbonate buffer, pH 9.0, giving approx 70% solubility, which closely resembles the solubility of wild-type inclusions under similar conditions (data not shown). The 130-kDa solubilized mutant protoxins were also assessed for their proteolytic stability by digestion with trypsin, and all were found to produce two major trypsin-resistant products, of approx 47 kDa and 18 kDa, respectively, that were identical to products of the wildtype toxin (Fig. 2, lanes 1-4). These results suggested that the point mutations in the loop residues of the mutant toxins had no apparent effect on proteolytic processing or protein folding.

To determine an effect of the loop mutations on toxicity, we tested *E. coli* cells expressing each type of the mutant toxin for their relative biologi-

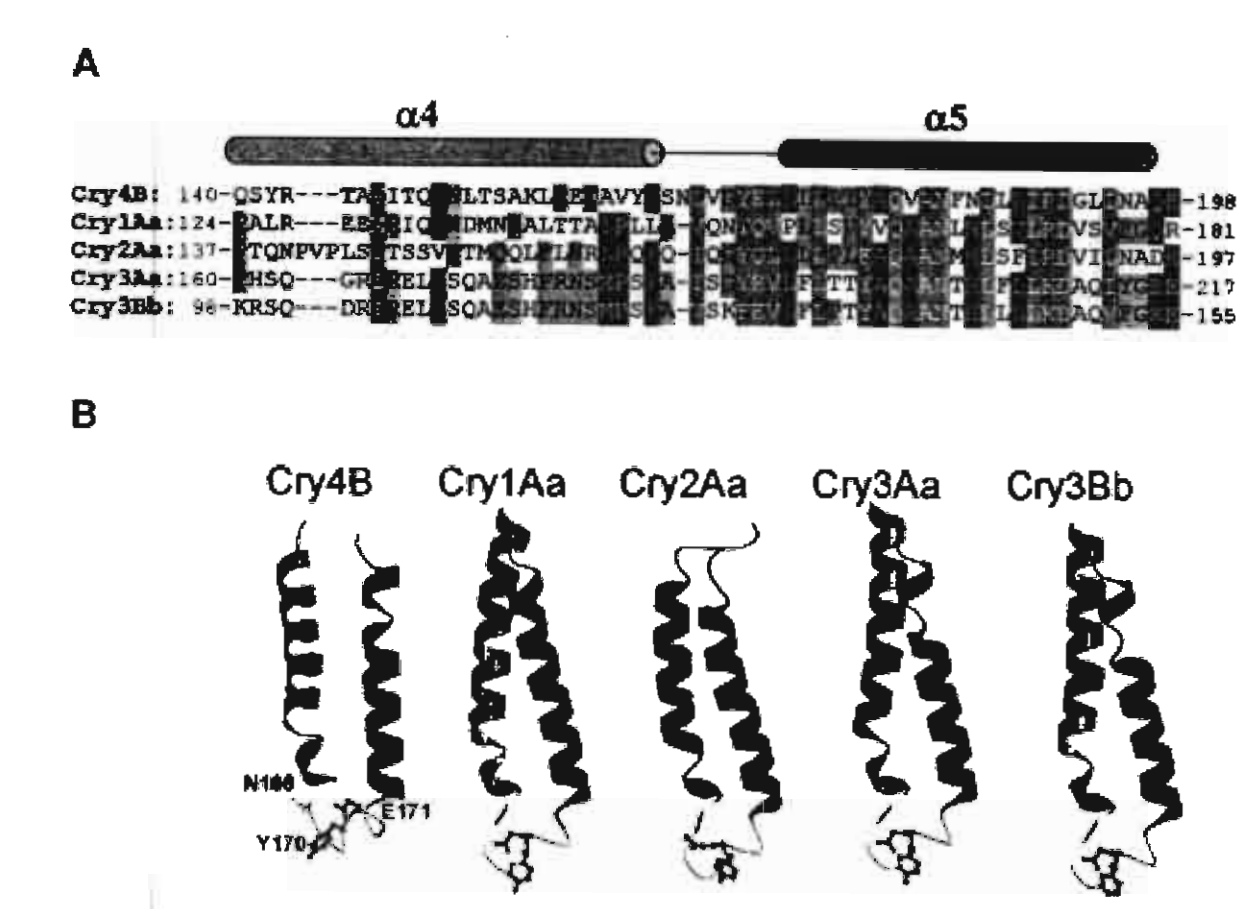


Fig. 1. (A) Multiple sequence alignment of the transmembrane α4-loop-α5 fragment of Cry4B with those of the known structures of Cry1Aa, Cry2Aa, Cry3Aa, and Cry3Bb toxins. The sequences were aligned using the program CLUSTALX. (B) Side views of the α4-loop-α5 helical hairpins of a homology-based Cry4B model and Cry1Aa, Cry2Aa, Cry3Aa, and Cry3Bb crystal structures. Grey ribbons represent helix 4 and helix 5. Balls and sticks show the mutated residues in Cry4B comparison with Cry1Aa, Cry2Aa, Cry3Aa, and Cry3Bb. Asn-166 is shown in Cry4B. Two relatively conserved loop-residues, Tyr and Glu or Gln, are shown in all five helical hairpins.

cal activity against 2-d old A. aegypti larvae. All bioassays were conducted in 10 replicas for each sample, and were repeated at least three times. The mortality data recorded after a 24-h incubation are shown in Fig. 3. Alanine substitutions of Asn-166 and Tyr-170 almost completely abolished the Cry4B bioactivity, although mutation at Glu-171 produced only a small decrease in larvicidal activity. These results suggested that Asn-166 and Tyr-170 play an important role in the larvicidal activity of the Cry4B toxin.

Further substitution of Asn-166 with Asp, Gln, Arg, Cys, or Ile, revealed that substitutions of Asn-166 with polar amino acids could preserve more than 80% of the toxicity of the wild-type

toxin, whereas substitution with a nonpolar residue (i.e., isoleucine) almost totally abolished the toxicity (see Fig. 3). All of the Asn-166-mutant toxins were tested for toxin stability, which revealed that all produced stable, trypsin-resistant products, as shown for some of these mutants in Fig. 2 (lanes 6 and 7). These results suggested that the polarity at position 166 in the α4-α5 loop is important for larvicidal activity of the Cry4B toxin. Molecular modeling of a putative toxin-induced pore consisting of six copies of the α4-α5 helical hairpin of Cry4B (see Fig. 4A) indicated that Asn-166 points toward the pore lumen and could form hydrogen bonds with water molecules. A crucial role in the mechanism of toxicity at this

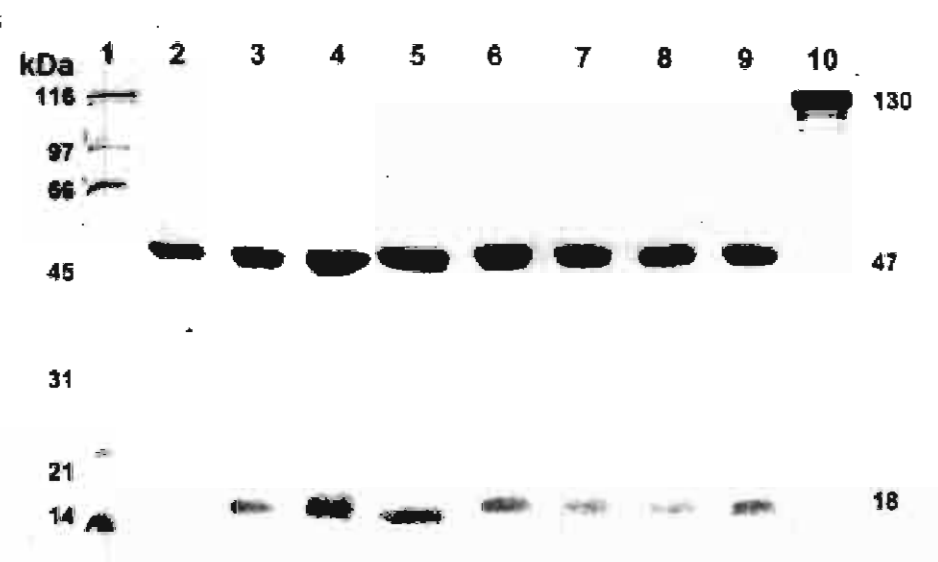


Fig. 2. SDS-PAGE (12.5% gel) analysis of proteolytic processing of Cry4B and its mutant toxins. *Lane 1*: molecular mass standards, *Lanes 2* and *10*: trypsin-treated products and the 130-kDa protoxin of wild-type Cry4B, respectively. *Lanes 3-9*: mutant representatives, consisting of N166A, Y170A, E171A, N166I, N166D, Y170D, and Y170F, respectively, after digestion with trypsin.

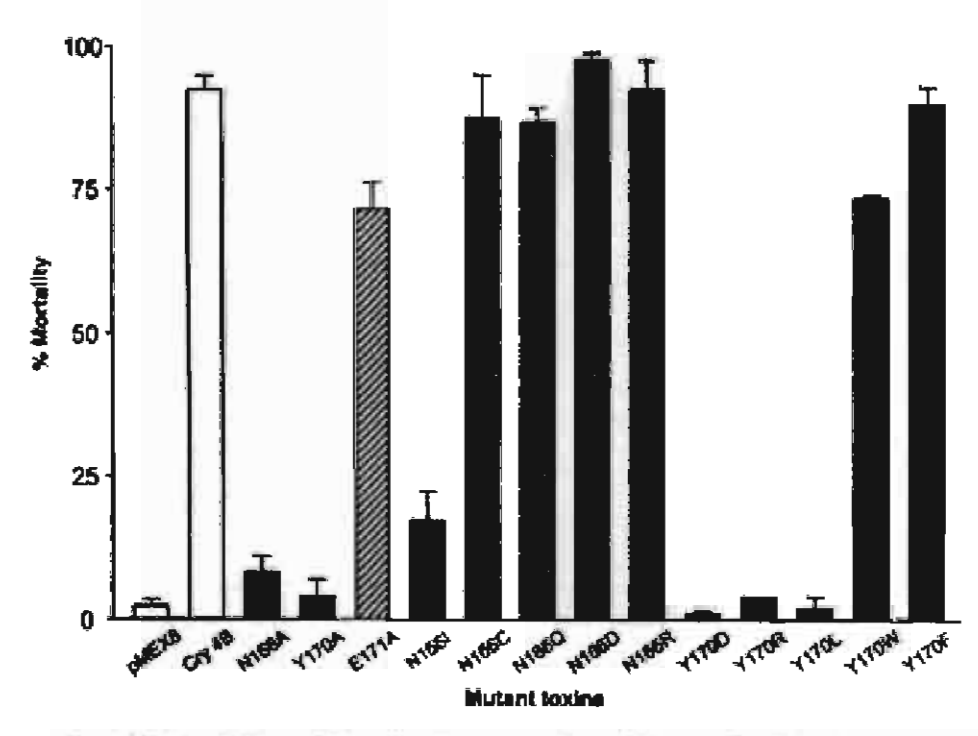


Fig. 3. Mosquito-larvicidal activities of *E. coli* cells expressing wild-type Cry4B toxin or mutant toxins (N166A, Y170A, E171A, N166I, N166C, N166Q, N166D, N166R, Y170D, Y170R, Y170L, Y170W, and Y170F) against *A. aegypti* larvae. Error bars indicate standard errors of the mean from three independent experiments.

critical position could conceivably be the formation of hydrogen bonds with water to stabilize the loop structure, or involvement in the passage of ions through the channel (see Fig. 4A). Whether these possibilities can be generalized remains to be elucidated.

Tyr-170 was also converted to Asp, Arg, Leu, Trp, or Phe. Interestingly, substitutions of this

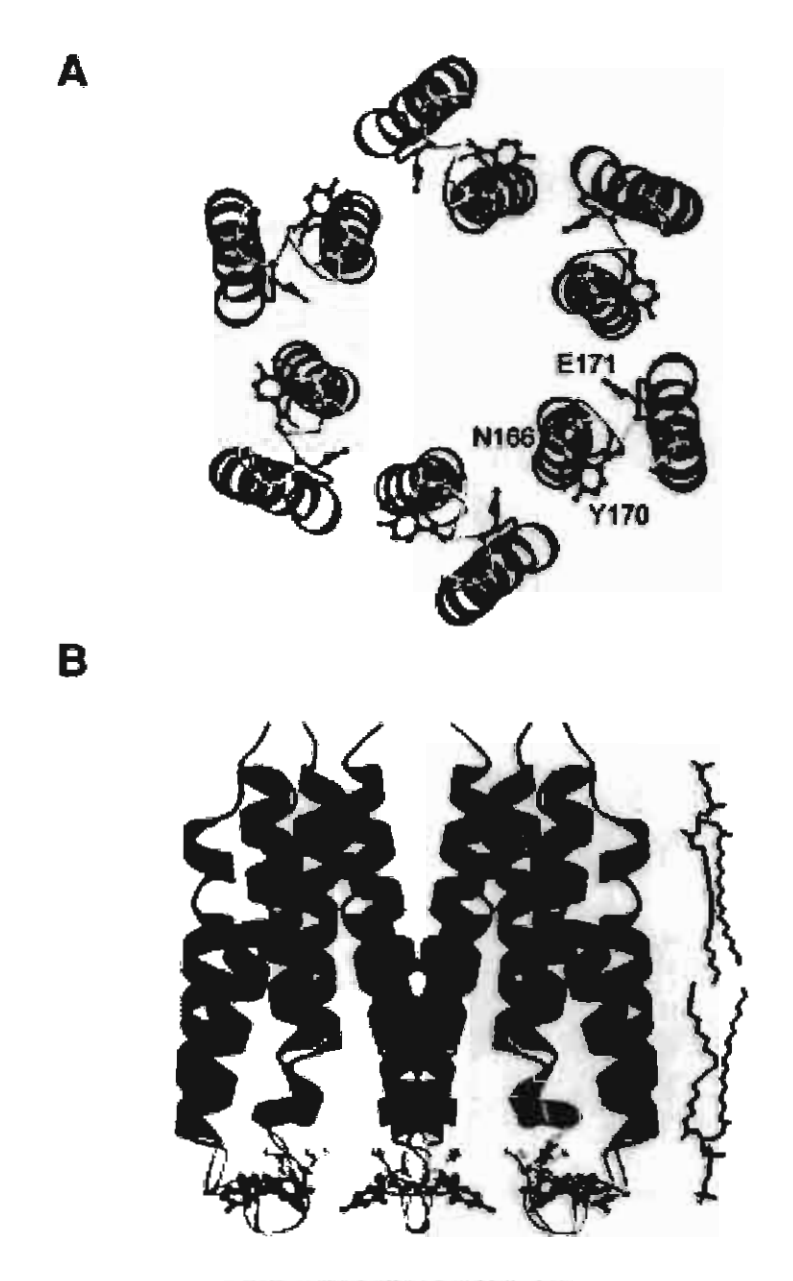


Fig. 4. (A) Bottom view of the model of a putative oligomeric pore consisting of six copies of the α4–α5 hairpin of the Cry4B toxin. Asn-166, Tyr-170, and Glu-171 are shown as balls and sticks. (B) The Tyr-170 residues are found at the membrane-water interface after oligomerization and pore formation. Rectangular boxes represent the planar lipid-membrane bilayers. Helices 4 and 5 are shown as grey ribbons.

critical tyrosine residue with only the aromatic residues (Trp or Phe) were shown to preserve Cry4B toxicity against mosquito larvae (see Fig. 3). Also, the protein expression levels, inclusion solubility, and proteolytic stability of the three other inactive mutants (Y170D, Y170R, and Y170L) suggested that their observed drastic loss of toxic-

ity is unlikely to be caused by misfolding of the protein. These results, together with the high level of conservation of the tyrosine residue at this position among the Cry toxins, strongly implies a general requirement for an aromatic structure at this crucial position. In several membrane proteins, a variety of roles have been proposed for

the aromatic residues, especially around Trp in the transmembrane helices, which are preponderantly found at or near the membrane water interface (23-25). These roles include to cilitating translocation of the periplasmic portion of proteins through the membrane, acting an determinants of protein orientation (26), introducing rigidity to the periphery of the transmembrane segments (27), or allowing vertical mobility of the transmembrane helical region with respect to the membranes (28). Considering all of the above. In an amount of the transmembrane helical region with the above. In an appropriate to the membranes (28). The periphery of the transmembrane helical region with respect to the membranes (28). Considering all of the above. In an appropriate to the membranes (28). The period of the protein for the period of the period of

In conclusion, our results indicate that the characteristics of polarity and aromamicity for residues at positions 166 and 170, respectively, in the $\alpha4-\alpha5$ loop play a crucial role in transity of the 130-kDa Cry4B toxin. However, turnier studies are needed to determine the exact tole of these two critical residues in toxin function.

Acknowledgmenes

The authors are grateful to Proc. Prapon Wilairat and Drs. A. Ketterman, C. Krittanai, P. Boonsenn, and B. Promdonkoy for their hamful comments. We also thank U. Chanama for an ellent technical support with DNA sequencing, and A. Nirachanon and S. Shimwai for technical assessance. This work was supported in part by the Thailand Research Fund through grants to C.A. and S.P. A Royal Golden Jubilee PhD research scholarship to Y.K. is gratefully acknowledged.

References

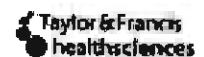
- Schnepf, E., Crickmore, N., V.E. Rie, J., Lereclus, D., Baum, J., Feitelson, J., et ... (1998). Bacillus thuringiensis and its pestician crystal proteins. Microbiol. Mol. Biol. Rev. 62. —806.
- de Maagd, R. A., Bravo, A., and Tickmore, N. (2001). How Bacillus thuringiensis has a volved specific toxins to colonize the insect work. Trends Genet. 17, 193-199.
- Hofje, H. and Whiteley, H. R. (489). Insecticidal crystal proteins of Bacillus the motensis. Microbiol. Rev. 153, 242-255.
- Crickmore, N., Zeigler, D. R., Fernelson, J., Schnepf, E., Van Ric, J., Lereclus, D., et a. 1998). Revision of the nomenclature for the Bacilla. Juningiousis pesti-

- cidal crystal proteins, Microbiol, Mol. Biol. Rev. 62, 807-813.
- Knowles, B. H. and Ellar, D. J. (1987). Colloid-osmotic lysis is a general feature of the mechanism of action of *Bacillus thuringiensis* delta endotoxin with difference insect specificity. *Biochim. Biophys. Acta.* 924, 509-518.
- Grochulski, P., Masson, L., Borisova, S., Pusztai-Carey, M., Schwartz, J. L., Brousseau, R, et al. (1995). Bucillus thuringiensis CrylA(a) insecticidal toxin: crystal structure and channel formation. J. Mol. Biol. 254, 447-464.
- Morse, R. J., Yamamoto, T., and Stroud, R. M. (2001). Structure of Cry2Aa suggests an unexpected receptor binding epitope. Structure (Camb.). 9, 409

 –417.
- Li, J. D., Carroll, J., and Ellar, D. J. (1991). Crystal structure of insecticidal delta-endotoxin from Bacillus liuringiensis at 2.5 Å resolution. Nature, 353, 815–821.
- Galitsky, N., Cody, V., Wojtezak, A., Ghosh, D., Luft, J. R., et al. (2001). Structure of the insecticidal bacterial delta-endotoxin Cry3Bb1 of Bacillus thuringiensis. Acta Crystallogr. [D. Biol. Crystallogr.] 57, 1101–1109.
- Uawithya, P., Krittanai, C., Katzenmeier, G., Leetachewa, S., Panyim, S., and Angsuthanasombat, C. (1999). Abstract. 32nd Meeting of the Society for Invertebrate Pathology, p.75.
- Von Tersch, M. A., Slatin, S. L., Kulesza, C. A., and English, L. H. (1994). Membrane-permeabilizing activities of *Bacillus thuringiensis* coleopteran-active toxin CryIIIB2 and CryIIIB2 domain I peptide. *Appl. Environ. Microbiol.* 60, 3711-3717.
- Walters, F. S., Slatin, S. L., Kulesza, C. A., and English, L. H. (1993). Ion channel activity of N-terminal fragments from CrylA(c) delta-endotoxin. Biochem. Biophys. Res. Commun. 196, 921-926.
- Punthecranurak, T., Leetachewa, S., Katzenmeier, G., Krittanai, C., Panyim, S., and Angsuthanasombat, C. (2001). Expression and biochemical characterization of the Bacillus thuringiensis Cry4B alpha1-alpha5 poreforming fragment. J. Biochem. Mol. Biol. 34, 293-298.
- Gazit, E., La Rocca, P., Sansom, M. S., and Shai, Y. (1998). The structure and organization within the membrane of the helices composing the pore-forming domain of Bacillus thuringiensis delta-endotoxin are consistent with an "umbrella-like" structure of the pore. Proc. Natl. Acad. Sci. USA 95, 12289-12294.
- Schwartz, J. L., Juteau, M., Grochulski, P., Cygler, M., Prefontaine, G., Brousseau, R., et al. (1997) Restriction of intramolecular movements within the Cry1Aa toxin molecule of *Bacillus thuringiensis* through disulfide bond engineering. FEBS Lett. 410, 397–402.
- Masson, L., Tabashnik, B. E., Liu, Y. B., Brousseau, R., and Schwartz, J. L. (1999). Helix 4 of the Bacillus thuringiensis Cry1Aa toxin lines the lumen of the ion channel. J. Biol. Chem. 274, 31996–32000.
- Nunez-Valdez, M.-E., Sanchez, J., Lina, L., Guereca, L., and Bravo, A. (2001) Structural and functional stud-

- ies of α-helix 5 region from Bacillus thuringiensis Cry1Ab δ-endotoxins. Biochim. Biophys. Acta. 1546, 122–133.
- Gerber, D. and Shai, Y. (2000). Insertion and organization within membranes of the delta-endotoxin pore-forming domain, helix 4-loop-helix 5, and inhibition of its activity by a mutant helix 4 peptide. J. Biol. Chem. 275, 23, 602-23607.
- Uawithya, P., Tuntitippawan, T., Katzenmeier, G., Panyim, S., and Angsuthanasombat, C. (1998). Effects on larvicidal activity of single proline substitutions in alpha 3 or alpha 4 of the Bacillus thuringiensis Cry4B toxin. Biochem. Mol. Biol. Int. 44, 825–832.
- Sramala, I., Leetachewa, S., Krittanai, C., Katzenmeier, G., Panyim, S., and Angsuthanasombat, C. (2001). Charged residues screening in helix 4 of the Bacillus thuringiensis Cry4B toxin reveals one critical residue for larvicidal activity. J. Biochem. Mol. Biol. Biophys. 5, 219-225.
- Sramala, I., Uawithya, P., Chanama, U., Leetachewa, S., Krittanai, C., Katzenmeier, G., et al. (2000). Single proline substitutions of selected helices of the Bacillus thuringiensis Cry4B toxin affect inclusion solubility and larvicidal activity. J. Biochem. Mol. Biol. Biophys. 4, 187–193.
- Angsuthanasombat, C., Chungjatupornchai, W., Kertbundit, S., Luxananil, P., Settasatian, C., Wilairat, P., et al. (1987). Cloning and expression of 130-kd mosquito-larvicidal delta-endotoxin gene of Bacillus

- thuringiensis vat. israelensis in Escherichia coll. Mol. Gen. Genet. 208, 384–389.
- Doyle, D. A., Morais, C. J., Pfuetzner, R. A., Kuo, A., Gulbis, J. M., Cohen, S. L., et al. (1998). The structure of the potassium channel: molecular basis of K* conduction and selectivity. Science 280, 69-77.
- Yuen, C. T., Davidson, A. R., and Deber, C. M. (2000). Role of aromatic residues at the lipid-water interface in micelle-bound bacteriophage M13 major coat protein. *Biochemistry* 39, 16155–16162.
- Landolt-Marticorena, C., Williams, K. A., Deber, C. M. and Reithmeier, R. A. (1993). Non-random distribution of amino acids in the transmembrane segments of human type I single span membrane proteins. J. Mol. Biol. 229, 602-608.
- Schiffer, M., Chang, C. H., and Stevens, F. J. (1992).
 The functions of tryptophan residues in membrane proteins. *Protein Eng.* 5, 213-214.
- Tsang, S. and Saier, M. H., Jr. (1996). A simple flexible program for the computational analysis of amino acyl residue distribution in proteins: application to the distribution of aromatic versus aliphatic hydrophobic amino acids in transmembrane alpha-helical spanners of integral membrane transport proteins. J. Comput. Biol. 3, 185–190.
- Pawagi, A. B. and Deber, C. M. (1990). Ligand-dependent quenching of tryptophan fluorescence in human erythrocyte hexose transport protein. *Biochemistry* 29, 950-955.



lon channels formed in planar lipid bilayers by the dipteran-specific Cry4B Bacillus thuringiensis toxin and its $\alpha1-\alpha5$ fragment

Theerapom Puntheeranurakt, Panapat Uzwithyat, Lána Potvint, Chanan Angauthanasombatt and Jean-Louis Schwartzi§*

- † Laboratory of Molecular Biophysics, Inatitute of Molecular Biology and Genetics, Mahidol University, Salaya Campus, Nakompathom 73170, Thailand
- ‡ Biotechnology Research Institute, National Research Council of Canada, 6100 Royalmount Avenue, Montreal, Quebec H4P 2R2, Canada
- § Groupe d'étude des protéines membranaires, Université de Montréal, PO Box 6128, Centre-Ville Station, Montreal, Quebec H3C 3J7, Canada

Summary

Trypain activation of Cry4B, a 130-kDa Bacillus thuringiansis (Bt) protein, produces a 65-kDs toxin active against mosquito larvee. The active toxin is made of two protease-resistant products of ca. 45 kDs and ca. 20 kDa. The cloned 21-kDs fragment consisting of the M-terminal region of the to:dn was previously shown to be capable of permeabilizing liposomes. The present study was designed to test the following hypothesse: (1) Cry4B, like several other St toxins, is a channel-forming toxin in planer lipid bilayers; and (2) the 21-kDs Nterminal region, which maps for the first five helices (al-a5) of domain 1 in other Cry toxins, and which putetively shares a similar tri-dimensional structure, is sufficient to account for the ion channel activity of the whole toxin. Using circular dichrolam spectroscopy and planar lipid bilayers, we showed that the 21kDa polypeptide existed as an a-helical structure and that both Cry4B and its at -25 fragment formed ion channels of 248 ± 44 pS and 207 ± 23 pS, respectively. The channels were cation selective with a polassium-to-chloride permeability ratio of 6.7 for Cry4B and 4.5 for its fragment. However, contrary to the fulllength toxin, the $\alpha 1-\alpha 5$ region formed channels at low dose; they tended to remain locked in their open state and displayed flickering activity bouts. Thus, like the full-length toxin, the atα5 region is a functional channel former. A ph-dependent, yet undefined region of the textin may be involved in regulating the channel properties.

Keywords: Secultus thuringlensis, 5-endotexin, truncated protein, planer fold bilayer, ion channet.

Introduction

Bacillus thuringiansis (Bt) is an endospore-forming becterium that produces larvicidal proteins (Cry and Cyt 5-endotoxins) as crystalline inclusions during sporulation [1]. These proteins are highly toxic to a wide variety of important insect pests as well as other invertebrates, which explains the extensive use of Bt as a biological control agent. To date, 40 classes of cry gene sequences have been identified based on their deduced amino acid sequence identity [2]. Upon ingestion by susceptible larvae, the proteic crystals are solubilized and proteolytically cleaved in the alkaline midgut juice to produce the activated toxins [1]. These, in turn, bind to specific receptors on the mid-gut epithelial cells and form pores in their membranes, resulting in cell swelling and eventually cell lysis due to comotic imbalance [3,4].

The 130-kDa Cry4A and Cry4B protoxins produced by 8t aub-species israelensis are toxic, following solub ization and proteolytic processing in the insects' gut, to Aedes aegypti, Anopheles gemblee and Culex quinquefasciatus moequito larvae [5]. These mosquitoes are serious human disease vectors that transmit malaria, filarial parasites, dengue and yellow fever virus. The exact mode of action of Cry4 toxins is not known. It has been proposed that most Cry toxins share a similar folding based on the five highly conserved regions of their primary amino acid sequences. This is supported by the fact that the atomic resolution crystal structures obtained for Cry1Aa [8], Cry2Aa [7], Cry3A [8] and Cry3Bb1 [9] toxins are very similar. In vitro proteolysis of the full-length Cry4A and Cry4B protoxins produces activated toxins that are composed of two non-covalently associated fragments resulting from the cleavage of the loops between helices at and at [5,10], as deduced from three-dimensional models of Cn/4A and Cry48 generated by homology modelling (unpublished data). This cleavage is critical for in vitro cytolytic activity [10].

Several activated Cry toxins, including Cry1Aa [6,11-14], Cny1Ac [13,15-17], Cny1B [13], Cny1C [18], Cny2A [19], Cry3As [16] and Cry3B2 [20], have the ability to form ion channels in receptor-free phospholipid vesicles and planar lipid bilayer membranes. Different Cry toxins have conductances ranging from a few pS to over 1000 pS, suggesting that certain Cry classes might have specific channel characteristics. Since the N-terminal domain of Cry toxins, which is made of seven to eight helices, is thought to play a crucial role in membrane insertion and pore formation [14,21-29], we hypothesized that the first five helices of the Cry4B toxin may constitute the putative pore-forming region responsible for membrane permeabilization by this toxin. This is supported by the fact that Cry4B helices 4 and 5 play an important role in mosquito larvicidal activity [28,30] and that the $\alpha 1 - \alpha 5$ fragment of the toxin permeabilizes liposomes [31]_

In this study, ion channel formation by the activated Cry4B toxin and its $\alpha 1 - \alpha 5$ fragment was investigated. The results show that both form cation-selective channels that have different properties under identical pH conditions. Therefore, while the $\alpha 1 - \alpha 5$ region is sufficient to account for the permeabilizing effect of the whole toxin, the overall channel activity of the toxin is also dependent on a gating region that may have different properties depending on the pH condi-

^{*}To whom correspondence should be addressed. e-mail: jesn-louis.schwartz@umonfreal.ca

T. Puntheeranurak et al.

tions under which the protoxin has been processed and may map for a part of the activated toxin located outside its $\alpha 1 - \alpha 5$ region.

Results

Cry4B and #1 -#5 secondary structures

The secondary structures of the 65-kDa activated Cry48 toxin and its α 1- α 5 fragment were examined by circular dichroism spectroscopy. Figure 1 shows the CD spectra of Cry48 and the α 1- α 5 polypeptide in the 185-280-nm region. Since a negative band at about 222 nm is typical of α -helix content due to the nx* transition, the helical content was interpreted by the molar ellipticity at this wavelength. The activated Cry4B toxin and the α 1- α 5 fragment exhibited helical content values of 33% and 61%, respectively. These values are close to those calculated with the Swiss PD6 software used to model the full-length toxin and its α 1- α 5 peptide [32], i.e. 31% and 63%, respectively.

Channel properties of Cry4B and its at -a5 region

Under symmetrical conditions, Cry4B channel activity was observed after about 1 hour following addition of 150–300 nM of the toxin, whereas the channels formed by the $\alpha1-\alpha5$ region of the toxin were observed after a few minutes (never more than 30 min) at doses as low as 4.3 nM. Representative current traces of Cry4B and $\alpha1-\alpha5$ channels are shown in Figures 2(A) and 3(A) respectively.

The Cry4B toxin, solubilized and activated at pH 10.5, displayed multiple amplitudes with some steps occurring from the closed state, i.e. from I = 0, and showed many sub-

conducting states. In all Cry48 experiments, the current-Voltage relations were rectilinear (Figure 2(C)), demonstrating the ohmic behaviour of the channels. The channel conductances, obtained by Method 1 described in the Experimental procedures, ranged from 19 ± 4 to 399 ± 44 pS (Table 1). When all the ourrent steps were analysed (Method 3 in Experimental procedures), the conductances were found to be between 27 ± 10 and 248 ± 44 pS (Table 1). Fast kinetic activity was observed in a few experiments at some applied voltages (Figure 2(8)). Ion selectivity was measured by conducting experiments under asymmetrical conditions. The reversal potential, V_R, of the Cry48 channels was -20 ±2 mV (Table 1). Under the same lonic gradient conditions, the Nernst potential for K+, calculated at 25°C, was -28.2 mV, demonstrating the cation selectivity of the channels. The PK/PC permeability ratio was calculated using the Goldman-Hodgkin-Katz equation and the V_R value above. It was equal to 6.7, confirming the cationic selectivity of the Cry4B channels.

Unlike Cry4B, the α 1- α 5 fragment of the toxin could not be solubilized in 50 mM Na₂CO₃ buffer, pH 10.5, so 50 mM Tris buffer, pH 8.8, was used instead. In all experiments, some of the α 1- α 5 channels remained always open. Their current-voltage curves were rectilinear and their conductances, determined by Method 2 in Experimental procedures, ranged from 148 to 3243 pS (Figure 3(C) and Table 1). The conductances of all the current steps were between 35 \pm 4 and 207 \pm 23 pS (Table 1). At a 430-nM dose, the α 1- α 5 channels had very large conductances (in excess of 650 pS, and often larger than 1000 pS), quite larger than those of Cry4B, which were found to be in the 20-400-pS range, at similar doses, when the full-length toxin had been prepared at pH 10.5 (Table 1). To exclude the possibility that the large

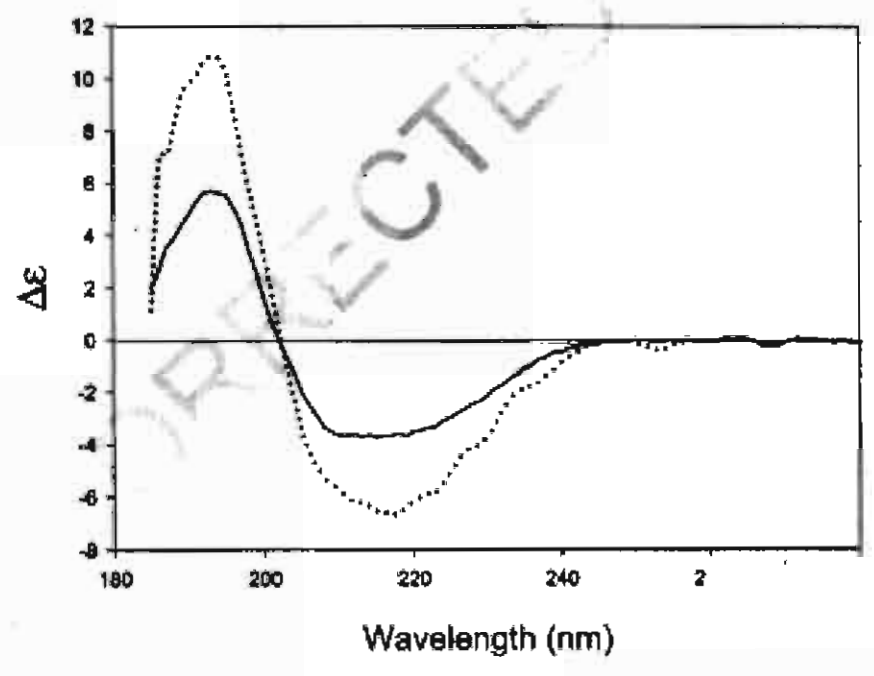
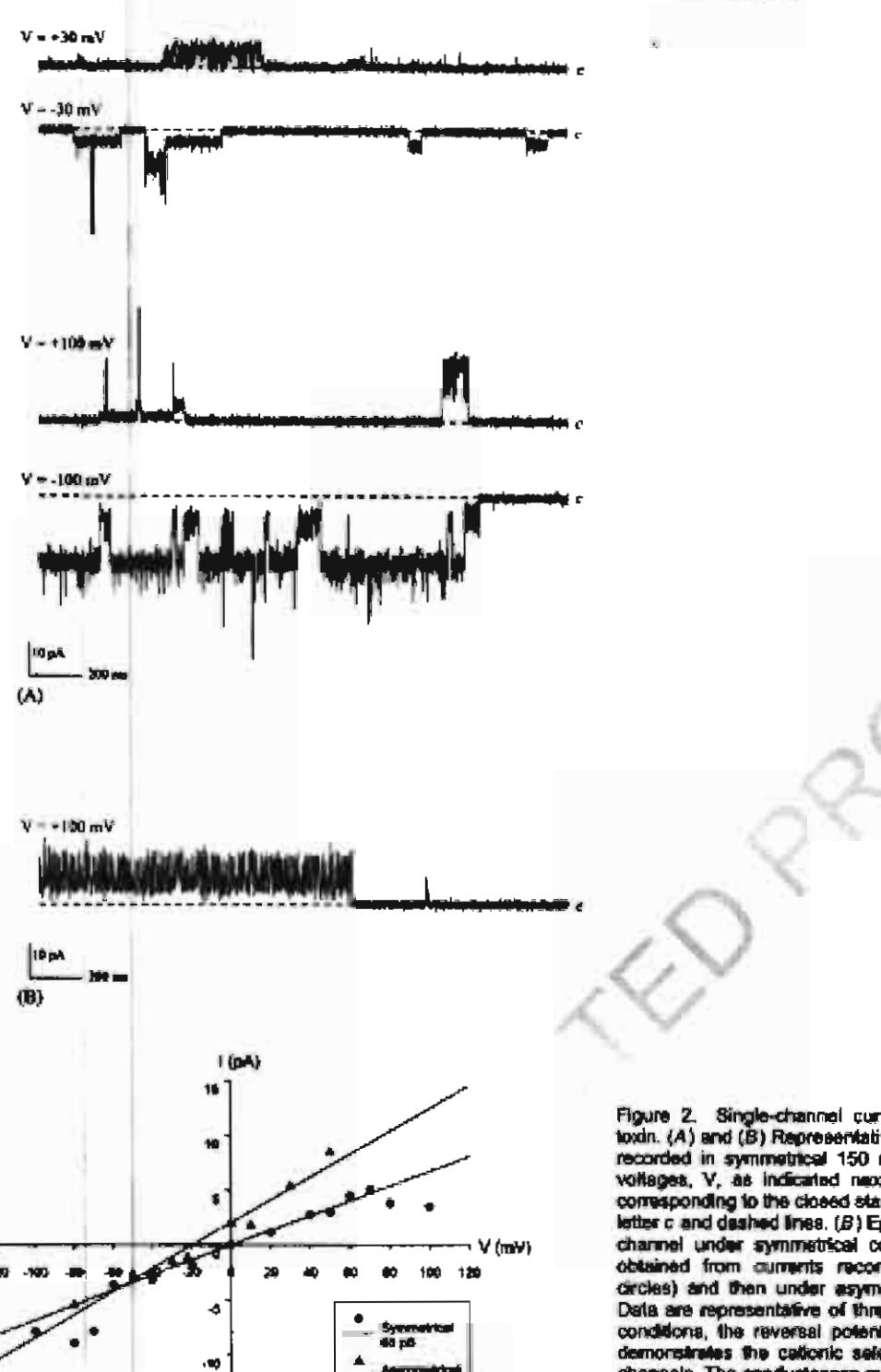


Figure 1. For UV circular dichroism spectra of the 85-kDa activated Cry48 toxin and its α 1 – α 5 polypeptide. The CD spectra of Cry48 (n = 3) in 10 mM NaH₂PO₄, pH 9.0, and the α 1 – α 5 fragment (n = 5) in 50 mM Tris, pH 8.8, are shown by dotted and solid lines, respectively. Ellipticity units (Δx , vertical scale) are per residue motar ellipticity.

Chairnels of full-length and fruncated Bt toxins



 $\alpha 1-\alpha 5$ channels corresponded to the superposition of several smaller channels with a very high probability of opening, smaller $\alpha 1-\alpha 5$ polypeptide concentrations were used, i.e. doses from 4.3 to 8.6 nM. Channel activity was still observed under these reduced dose conditions. Two differ-

(C)

Figure 2. Single-channel current traces of the activated Cry48 toxin. (A) and (B) Representative segments of typical current traces recorded in symmetrical 150 mM KCl solution at various holding voltages, V, as indicated next to the traces. The current levels corresponding to the closed state of all channels are indicated by the letter c and dashed lines. (B) Episode of fast kinetic activity of Cry48 channel under symmetrical conditions. Current-voltage relations obtained from currents recorded first under symmetrical (solid circles) and then under asymmetrical conditions (solid triangles). Data are representative of three experiments. Under asymmetrical conditions, the reversal potential was shifted to —20 mV, which demonstrates the cationic selectivity of the activated Cry48 toxindemonstrates the conductances measured under each set of conditions are given in the text box shown on the graph. Data points were fitted by linear regression.

ent kinetic behaviours were observed in $\alpha 1-\alpha 5$ channels. In some experiments, several channels were active and their open probability was very high (Figure 3(A)). In other experiments, the open probability of the channels was smaller (Figure 3(B)). Fast kinetics was also displayed in

T. Puntheeranurak et al.

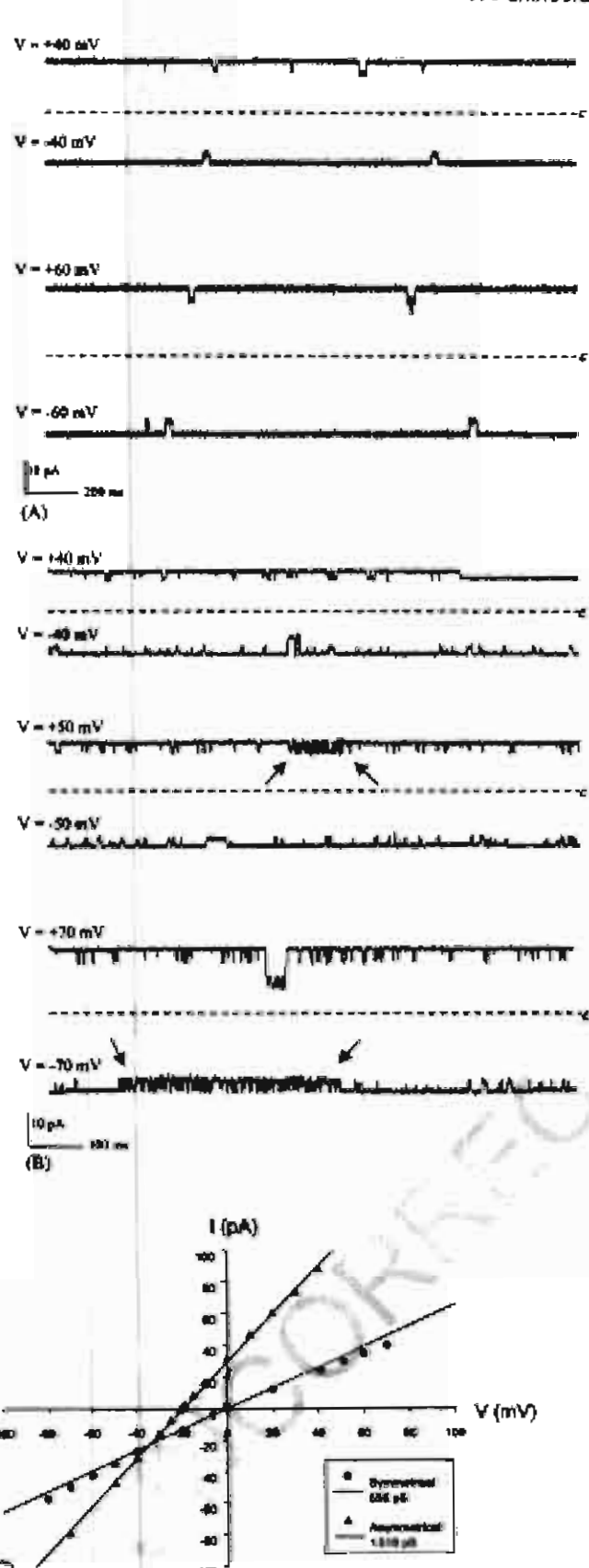


Figure 3. Single-channel current traces of Cry48's α1 – α5 fragment channels. (A) and (B) Representative segments of typical current traces recorded under 150 mM KCI symmetrical conditions at various holding voltages, V, as shown next to the traces. The current levels corresponding to the closed state of all channels are indicated by the letter c and dashed lines. (A) Representative records of channels displaying a very high open probability. Note that there are at least four identical channels solve in this experiment, with at least three channels simultaneously locked in their open states. (B) Representative records showing channel activity with average open probability and flictering behaviour (shown between arrows). At least five channels were active in this experiment, with at least two channels simultaneously locked in their open states. (C) Current—voltage relations obtained from currents recorded first under symmetrical (solid circles) and then under asymmetrical conditions (solid triangles). Data are representative of three experiments. Under asymmetrical conditions, the reversal potential was shifted to — 19 mV, which shows the cationic selectivity of the α1-α5 fragment channels, similar to that of the full-length toxin. The conductances measured under each set of conditions are given in the text box shown on the graph. Data points were fitted by linear regression.

Channels of full-length and truncated Bt toxins

Biophysical properties of the ion chamine's formed by the activated Cry48 tools and its of -of fragment.

Channel properties	Activated Cry48**	a1-a5 fragment*,b
Conductanosas	Calculation method ² 19 ± 4 ($n = 4$) 79 ± 8 ($n = 3$) 141 ± 1 ($n = 5$) 399 ± 44 ($n = 3$)	Calculation method* 148 $(n-1)$ 233 \pm 13 $(n=2)$ 412 \pm 14 $(n=4)$ 681 \pm 13 $(n=4)$ 790 \pm 14 $(n=4)$ 1014 \pm 16 $(n=5)$ 1529 \pm 9 $(n=2)$ 1794 $(n=1)$
Minimum and maximum conductances obtained from all observed current steps e,r V_H , reversel potential $(mV)^P$ P_K/P_{GI} , permeability ratio	$27 \pm 9 \ (n = 14)$ $248 \pm 44 \ (n = 14)$ $-20 \pm 2 \ (n = 11)$ 8.7	3243 $(n = 1)$ 35 ± 4 $(n = 19)$ 207 ± 23 $(n = 19)$ - 17 ± 1 $(n = 12)$ 4.5

^{*}mean ± SEM

*experiments were conducted under asymmetrical KCI conditions

three experiments, but not all every applied voltage (Figure 3(8), arrows). Under asymmetrical conditions, the $\alpha 1 = \alpha 5$ fragment formed cation-selective channels with V_R equal to 17 ±1 mV and a P_{IC}/P_{CI} permeability ratio of 4.5.

When the Cry4B protoxin was solubilized and activated at pH 9.0, it showed on 15% SDS-PAGE the same two major bands at about 47 kDa and 18 kDa as those seen with the toxin prepared at pH 10.5 (data not shown), but its channel activity was different. In all experiments, some of the channels remained always open, i.e. the current never returned to zero. The channels displayed multiple conductances varying from 16 pS to 3301 pS, similar to those observed with the $\alpha 1 - \alpha 5$ fragment (data not shown). On the other hand, the selectivity and the kinetic behaviour of the full-length toxin obtained from the Cry48 protoxin prepared at pH 9.0 did not differ from those of the toxin resulting from Cry4B solubilization and activation at pH 10.5 (data not shown).

Discussion

This study clearly demonstrates that the dipteran-specific Cry48 towin and its a1-a5 fragment form cation-selective channels in planar lipid bilayers, suggesting that the a1-a5 region is sufficient to form functional channels like those assembled by the full-length 65-kDa taxin. This concept is supported by previous studies that showed that the Nterminal domains of Cry1Ac, Cry3A and Cry3B2-I.e. the $\alpha 1 - \alpha 7$ regions of these toxins—form channels that compare well to those of the full-length loxins [20,33,34]. The present study provides the first evidence that the first five helices of a Cry totán can function efficiently as ion channels.

The incorporation time of the a1-a5 fragment into planer lipid blayers was faster than that of the full-length toxin and tower doses (4.3 nM) were required for the fragment to induce channel activity comparable to that of Cry48 and other Cry toxins, for which at least 70-150 nM are needed to induce activity. Furthermore, the $\alpha 1 - \alpha 5$ channel conductances were generally larger than those of the 65-kDa toxin (Table 1). It is conceivable that the $\alpha 1 - \alpha 5$ fragment, which is produced in aggregated form larger than 200 kDs, has a higher oligomerization order than the full-length toxin, which would explain the larger conductances observed. It is also possible that the smaller polypeptide is more flexible and requires a lesser conformational change to insert into the membrane, which would account for its faster integration into the membrane.

interestingly, the pH conditions used to solubilize and activate the 130-kDa Cry4B protoxin affected both the conductance range of the channels formed by the 65-kDs. toxin and their activity. When the protoxin was treated at pH 10.5, the conductance of the resulting toxin was found to be between 19 pS and 399 pS, and the channel currents did return completely to zero, whereas the range of the channel conductances of the 65-kDa toxin produced at pH 9.0 was far wider, i.e. from 16 pS to 3300 pS, and the channels never closed fully.

One simple explanation for the different kinetic behaviour of the full toxin and that of the $\alpha 1 - \infty 5$ polypeptide may be that the residues involved in the transition from the open state to the closed state of the Cry4B channels are located in a region of the toxin that is not mapped by the $\alpha 1 - \alpha 5$ polypaptide. Their absence in the truncated protein would therefore account for the tendency of the #1-#5 channels to remain open. However, when Cry48 was prepared at pH 9.0 rether than pH 10.5—a lower pH, which did not result in toxin truncation as demonstrated by the presence of the two major bands observed at about 47 kDa and 18 kDa on SDS-PAGE—its channel kinetic activity resembled that of the α1a5 polypeptide. Thus, it cannot be excluded that the residues involved in gating are located in the #1-#5 region itself and that, under the reduced preparative pH conditions used for

^{*}n indicates the number of experiments

experiments were conducted under symmetrical KCI conditions

conductances were determined using Method 1 (see Experimental procedures) conductances were determined using Method 2 (see Experimental procedures)

conductances were determined using Method 3 (see Experimental procedures)

T. Puntheersnurak et al.

the full toxin (pH 9.0) and its $\alpha 1-\alpha 5$ fragment (pH 8.8), the capacity of the gating residues to return the channels to the closed state was inhibited, which would explain the similar kinetic behaviour of Cry4B and its $\alpha 1-\alpha 5$ fragment under these conditions. This pH-dependence of the channel activity remains to be elucidated further.

Therefore, our results suggest that the pH at which the protoxin is processed affects the regions of the toxin involved in ofigomerization, cluster assembly and gating due to protonation or deprotonation of certain residues. There is evidence that perticular stretches in domain 3 of Cry1Aa and Cry1Ac toxins are involved in ion channel regulation [12,35]. Moreover, it has been reported that pH directly affects Cry1C channel selectivity and conductance [18] and that reducing pH promotes unfolding of this toxin [36], Furthermore, it has been shown recently that large conductances of Cry1C channels are actually due to clusters of channels of smaller conductances [37].

Taken together, our data demonstrate that the major determinant of Cry4B pore formation is the α 1- α 5 segment of the putative domain 1 of the toxin, a region that functions as an efficient channel-forming polypeptide without the remainder of the activated protein. Our results also show that Cry4B channel size and gating depends on the pH conditions used for the processing of the protoxin. While it is possible that assembly and gating of the channels are regulated by residues located outside the α 1- α 5 region of the toxin, it cannot be excluded that they may be found within the α 1- α 5 segment itself, in an area that is sensitive to pH during the processing of the truncated polypeptide and the 136-kDa protoxin. Further work is needed to locate this particular region of the Cry4B protein and to clarify the rote of pH in its gating and pore-assembly properties.

Experimental procedures

Toxin preparation

Cry4B proteins and the α 1- α 5 polypeptides were expressed as inclusion bodies produced from the cloned cry4B and α 1- α 5 genes in E. co9. They were partially purified as described earlier [31], Cry4B was solublized and then trypain-activated in 50 mM Na₂CO₃, pH 9.0 or 10.5, except for secondary structure determination where 10 mM NaH₃PO₄, pH 9.0, was used instead. Protein concentrations were determined using a Bio-Rad protein quantitative kit with bowine serum efforms (Sigma-Aldrich Corp., St Louis, MO, USA) as a standard. The activated Cry4B toxin was further purified by size-exclusion chromatography using a Superose 12 column (Amerikam Bloscienoss Corp., Piscataway, NJ, USA). The punified fractions were analysed by SDS-15% w/y polyacryamide gel electrophoresis. Purified Cry4B came out as a monomeric form with its two fragments of 47 kDa and 21 kDa attached together.

Since the a1-a5 fragment could not be solubilized in 50 mM Na₂CO₃ buffer, pH 10.5, 50 mM Tris buffer, pH 8.8, was used. The solubilized protein was passed through a Centricon-10 (Milipore, Billerica, MA, USA) for concentrating before injection on a Superdex 200 FPLC column (Amersham Biosciences Corp., Piscetaway, NJ, USA). The protein was detected in the void volume as an aggregate larger than 200 kDa (data not shown). Prior to use, toxin solutions were vortected and sonicated for about 1 min to prevent aggregation.

Circular dichroism (CD) spectroscopy

CD spectra of the activated Cry48 town and the α 1 – α 5 polypeptide were measured with a Jasco J-715 spectropolarimeter (Jasco Inc., Easten, MD, USA). They were scanned between 185 nm and 280 nm at room temperature in a rectangular quartz curvette with a 0.2-mm optical path length. CD measurements of Cry48 (n=3) and its α 1 – α 5 fragment (n=5) were taken at a rate of 20 nm/mm. The concentration of the full-length tooln and its truncated polypeptide was equal to 4.5×10^{-5} M and 3×10^{-3} M, respectively, as determined by far UV absorbance. Spectra was corrected for solvent baseline obtained under the same conditions. The motor circular dichroism Δs at a given wavelength was calculated with the following formula:

 $\Delta s = (K \times \theta \times M_{\star})/(c \times N \times d)$

where K was equal to 3298×10^4 , θ was the measured ellipticity (in millidegrees), M, was the molecular weight of the sample, c was the sample concentration (in g/mi). N was the number of peptide bonds of the sample and d was the optical path length of the sample cell (in cm). Reference spectra were obtained and scale calibration at 290 nm was performed with camphorsulfonic acid (CSA, Sigma-Aldrich Corp., St. Louis, MO, USA) and the θ value of CSA (1 mg/ml) was measured at the beginning of each experiment, giving Δt (192.5 nm)/ Δt (290.5 nm) = 2.08 (38). The helical contents of the protein and its fragment were derived from their Δt determined at 222 nm using Δt (222 nm) = 10.5 as the value for 100% helicity (39).

Planar lipid bilayers

Planar lipid bilayers were formed from the 7:2:1 (wt/wt) lipid mixture of PE, PC and Ch [18]. The final concentration was 25 mg/ml dissolved in decane. The lipid bilayer was painted, using a pre-pulled glass pipette dipped in the decane-lipid solution, on a 200-um orifice drilled in a Delrin cup and pre-treated with the same lipid mixture. Membranes had a typical capacitance of 150-250 pF and remained stable for several hours. Before town or polypeptide reconstitution, the bilayer was monitored under non-zero holding voltage conditions for more than 30 min to groupe that no conteminant-induced charmel activity was present. Incorporation was performed by adding eliquots of the protein or its fragment directly to the cis chamber, which was stirred using a small magnetic flee until channel activity was observed. The insertion process was facilitated by applying a 100mV holding potential across the bilayer. Channel activity was detected by the presence of distinct current jumps recorded during test voltage steps applied across the planer lipid bilayer. Activated Cry48 was used at concentrations between 150 nM and 300 nM, whereas the a1-a5 fragment concentration ranged from 4.3 nM to 430 nM. All experiments were performed at room temperature (22-25°C).

Deta recording and analysis

Single channel currents were recorded with an Axopatch-1D patchclamp amplifier (Axon Instruments, Foster City, CA). Signate were digitized with a Digidata 1200 analogue-to-digital converter using Axoscope 8.0 software (both from Axon Instruments) at a 50-kHz sampling frequency. They were low-pass filtered at 600 Hz and analysed on a personal computer using Axoscope 8.0 software.

Channel conductances were determined as follows. In experiments where channel currents returned to the baseline—i.e. to the current level observed at any particular voltage in the absence of either the toxin or its fragment—the largest amplitude of the current steps observed from, or to, the baseline level was plotted against applied voltage to generate current-wittage relations, or I-V curves (Mathod 1). In experiments where channel currents never returned to the baseline—i.e. In which at least one channel remained always open—the main channel current was obtained from the amplitude of the smallest current level observable for at least 50% of the duration of the recording at each voltage, and the corresponding I-V curves were obtained (Method 2). Finally, all observable current steps were measured for each voltage and their amplitudes were plotted versus

voltage (Method 3). Using the three methods described above, the channel conductances were then derived from the slopes of the linear regression lines to the data points. The conductances obtained for each individual experiment were then averaged over the number of experiments performed under the same conditions. Results are expressed as means ± SEMs.

ion selectivity was measured under 450/150 mM KCI (cis/trans) asymmetrical conditions. The reversal potential, V_R , was obtained as the voltage for which the corresponding linear regression intersected the horizontal axis of the I-Y curves, and was compared to the value calculated for K* according to Nernst equation [40]. Channel selectivity for K* over Cl $^-$ was derived from P_K/P_{Cl} permeability ratios calculated using V_R and the Goldman-Hodgiún-Katz equation

Chemicals and solutions

Phosphatidylethanolamine (PE), phosphatidylcholine (PC) and chosterol (Ch) were obtained from Avanti Polar Lipida (Alabaster, AL, USA). All other chemicals used were of analytical grade (from verious suppliers). Under symmetrical conditions, both the cis and the trans chambers of the bilayer experimental apparatus contained 150 mM KCI, 1 mM CaCl2 and 10 mM Tris-HCI, pH 9.0. For ion selectivity determination, ionic gradients were established with 450 mM KCI on the cis side and 150 mM KCI in the trans side of the bileyer.

Acknowledgements

We are grateful to Professor Sakol Panyim, Professor Prapon Wilairat, Dr Gerd Katzenmeir, Dr Albert Kettermen and Dr Chartche Krittenei for helpful comments, and to W. Phetalchindachote, A. Bourchookam, U. Chanama and Maro Juteau for technical assistence. This work was supported in part by grants from the Thalland Research Fund to CA and the Natural Sciences and Engineering Research Council of Canada to JLS, and by the Thailand Research Fund - National Research Council of Canada scientific exchange programme to CA and JLS. A Golden Jubilee PhD research scholarship to TP is gratefully acknowledged.

References

[1] Höfte, H. and Whiteley, H. R., 1969, Insecticidal crystal proteins of Bacitius thuringiansis. Microbiol. Rev., 53, 242-255.

[2] Crickmore, N., Zeigier, D. R., Feitelson, J., Schnepf, E., Van Se, J., Lerectus, D., Baum, J. and Dean, D. H., 1998, Revision of the nomenciature for the Bacillus thuringlensis pesticidal crystal proteins, Microbiol, Mol. Biol. Rev., 62, 807-813.
[3] Knowles, B. H., 1994, Mechanism of action of Backlus

thuringlerusis insecticidal 6-endotoxins. Adv. Insect Physiot., 24, 275-308.

Schnepf, E., Crickmora, N., Van Rie, J., Leredius, D., Beum, J., Fehicison, J., Zeigler, D. R. and Deen, D. H., 1996, Sacultus thuringiansis and its peeticidal crystal proteins. *Microbiol. Mol. Biol. Rev.*, \$2, 775-806.

[6] Angeuthanesombat, C., Crickmore, N. and Ellar, D. J., 1992, Comparison of Bacillus thuringlarisis subsp. israelansis CryfVA and CryfVB aloned toxins revisals synergiam in vivo. FEMS

Microbiol Left., 73, 63-68.

[8] Grochulski, P., Masson, L., Bortsova, S., Pusztai Carey, M., Schwartz, J. L., Brouspeau, R. and Cygler, M., 1995, Bacillus thuringionals CrytA(a) insecticidal toxan: crystal structure and channel formation. J. Mol. Biol., 284, 447-464.

[7] Horse, R. J., Yamamoto, T. and Stroud, R. M., 2001, Structure of Cry2As suggests an unexpected receptor binding epitope. Structure, 8, 409-417.

(8) Li, J. D., Carroll, J. and Ellar, D. J., 1991, Crystal structure of insecticidal della-endotoxin from Bacillus thuringiansis al 2.5 Å resolution. Nature, 363, 815-821.

[9] Gellisky, N., Cody, V., Wojiczak, A., Ghosh, D., Luft, J. R. Pangborn, W. and English, L., 2001, Structure of the insecticidal becleriel delta-endotoxin Cry38b1 of Beciffue thuringiansis. Acta Crystallogr, D. Blot. Crystallogr., 57, 1101-1109.
[10] Angsuthanasombet, C., Crickmore, N. and Ellar, D. J., 1993,

Effects on toxicity of eliminating a cleavinge affe in a predicted internetical loop in Bealtus theringleness CrylVB detta-endo-

toxin. FEMS Microbiol. Left., 111, 255-261.

[11] Peyronnet, O., Vechon, V., Schwartz, J. L. and Laprade, R., 2001, Ion channels induced in planar lipid bilayers by the Becilius thuringlensis toolin Cryt. Aa in the presence of gypsy moth (Lymentife disper) brush border membrane. J. Membr. Biol., 184, 45-54.

[12] Schwartz, J. L., Potvin, L., Chen, X. J., Brousseau, R., Laprade, R. and Deen, D. H., 1997, Single-site mutations in the conserved alternating-arginine region affect ionic channels formed by CrylAs, a Becilius thuringlensis toxin. Appl. Environ.

Afterobiol., 53, 3978-3984. [13] Schwartz, J. L., Lu, Y. J., Schniein, P., Brousseau, R., Laprade. R., Masson, L. and Adang, M. J., 1997, Ion channels formed in planer lipid bileyers by Bacillus thuringiensis toxins in the presence of Menduce sexte midgut receptors. FEBS Lett., 412, 270-276.

[14] Schwartz, J. L., Juteau, M., Grochulski, P., Cygler, M., Préfontaine, G., Brousseau, R. and Masson, L., 1997, Restric-tion of intramolecular movements within the Cry1Aa toxin

molecule of Becilius thuringlensis through disulfide bond engineering. FEBS Lett., 410, 397–402.

[15] Chandra, A., Ghosh, P., Meridaokar, A. D., Bera, A. K., Sharme, R. P., Das, S. and Jumar, P. A., 1999, Amino acid substitution in alpha-halix 7 of Gry1An delta-endotedn of Bacilius thuringiensis leuds to enhanced toxicity to Helicoverpa armigere Hubner. FEBS Lett., 488, 175-179. [18] Stefin, S. L., Abrams, C. K. and English, L., 1990, Delte-

endoloxins form cation-selective channels in planar lipid

bilayers. Biochem Biophys. Res. Commun., 169, 765-772.

[17] Smedley, D. P. Armetrong, G. and Ellar, D. J., 1997, Channel activity caused by a Becilius thuringleness delta-endotoxin. preparation depends on the method of activation. Mot. Membr. Biol 14, 13-18,

[18] Schwartz, J. L., Germesu, L., Severia, D., Masson, L., Brousseau, R. and Rousseau, E., 1993, Lepidopteran-specific crystal toxins from Bacillus thuringlenais form cation- and anionselective channels in planar lipid bilayer. J. Membr. Biol., 132,

[19] English, L., Robbins, H. L., Von Tersch, M. A., Kulesza, C. A., Ave, D., Coyle, D., Jeny, C. S. and Statin, S. L., 1994, Mode of action of CryllA: a Becilius thuringlensis delta-endotoxin. Insect Biochem. Mol. Biol., 24, 1025-1035.

[20] Von Tersch, M. A., Slatin, S. L., Kulesza, C. A. and English, L. H., 1994, Membrane-permeabilizing activities of Becilius thuringrenals coleopteran-active toxin CrylliB2 and CrylliB2 domain I peptide. Appl. Emviron. Microbiol., 60, 3711-3717.

[21] Alcantara, E. P., Alzala, O., Lee, M. K., Curties, A. and Dean, D. H., 2001, Role of alpha-helix seven of Sectifus thuringlensis Cry1Ab della-endotoxin in membrane insertion, structural stability, and ion channel activity. Biochemistry, 40, 2540-2547.

[22] Amold, S., Curtiss, A., Dean, D. H. and Alzate, O., 2001, The role of a proline-induced broken-helix matif in alpha-helix 2 of Becilius thuringienals della-endotorers. FEBS Lett., 490, 70-

[23] Coux, F., Vaction, V., Rang, C., Monzar, K., Masson, L., Royer, M., Bes, M., Rivest, S., Brousseau, R., Schwartz, J. L., Legrade, R. and Frutos, R., 2001, Rote of Interdomain self. bridges in the pore-forming ability of the Backlus thuringle toxins Cry1Aa and Cry1Ac. J. Biol. Chem., 276, 35546-35551. [24] Dean, D. H., Rajamohan, F., Lee, M. K., Wu, S. J., Chen, X. J.,

Alcantara, E. and Hussain, S. R., 1996, Probing the mechanism of action of Baciflus thuringliensis insecticidal proteins by site-directed mutagenesis—a minimariew. Gene, 179, 111–117.

[25] Kurnar, A. S. and Aronson, A. I., 1999, Analysis of mutations in the pore-forming region essential for insecticidal activity of a